DOE/ER/45113--T3

DE92 007748

Performance Report
Superconducting Materials
September 1, 1991 - February 28, 1992
Grant No. DEFG05-84ER45113

J. Ruvalds
Department of Physics
University of Virginia
Charlottesville, VA 22901

Prepared for the Department of Energy under Grant No. DEFG05-84ER45113

DISCLAIMER

Table of Contents

		Page
Paper Published During Grant Period		1
Papers Submitted and Invited Talks During Grant Period		2
Personnel and Students		3
Time Devoted to Project by Principal Investigator		6
Research Projects		7
I.	Nested Fermi Liquid (NFL) Response in High Temperature Superconductors	8
II.	Optical Reflectivity and Electron Loss Data	11
III.	Electronic Raman Spectra	15
IV.	Neutron Scattering Cross Section and Scaling	18
V.	Prospects for New Superconductors	22
	References	24

Papers Submitted During Grant Period

1. "Neutron Spectra and Scaling in High Temperature Superconductors", J. Ruvalds, C. T. Rieck, J. Zhang, and A. Virosztek (submitted to Phys. Rev. Letters).

Lectures and Invited Talks in 1990

IBM Thomas J. Watson Research Center

Gordon Conference on Correlated Systems, Brewster, MA

Université Pierre et Marie Curie, Paris

Institut Laue-Langevin, Grenoble, France

Kernforschungscentrum, Karlsruhe, Germany

Walther-Meissner Institut, Garching, Germany

University of California at Irvine

University of California at Los Angeles

Lectures and Invited Talks in 1991

Workshop on Fermiology of High T_c Superconductors, Argonne, IL

University of Toronto

Los Alamos National Lab

Southeastern Section Meeting of the American Physical Society, Durham, NC

Personnel and Students

Dr. Carsten T. Rieck joined our group as a Research Associate on September 1, 1991 after earning a PhD degree at Hamburg University in Germany. His exceptionally strong background in theoretical physics has already resulted in new results for the neutron spectra of high temperature superconductors which have been submitted for publication.

Dr. Jian Zhang completed a one-year term as Research Associate with our group and moved on to a job as an environmental consultant with a company in Pittsburgh. His computer calculations of Fermi surface nesting effects in superconductors have been especially constructive.

Dr. A. Virosztek completed his postdoctoral appointment in the summer of 1990 and continues to work with our group on research projects involving high temperature superconductors. He now holds a permanent job in Budapest, Hungary and occasionally consults with the research group in Garching, Germany that is expert in Raman spectroscopy.

Graduate student Jeffrey Thoma joined our group this autumn. His undergraduate honor thesis at the University of Delaware employed sophisticated computational techniques.

In previous years our efforts to discover new superconductors involved the enthusiastic participation of students with various backgrounds and interests. In addition to graduate student Tom Sutto, the following undergraduate students contributed to our research: Gregory Ashe, (now grad student at U. Michigan); Hyun B. Shin (now grad student at U. Virginia); Mike Rilee (now grad student at Cornell); and undergraduates Sarah Woldehana, Clark Allen, Mike Diener, Peter Owen, Cynthia Vinion, and Vera Siregar.

We look forward to involvement of undergraduates as well as graduate students in the future.

Synopsis of Research by Personnel and Students

The research initiated with Research Associate Dr. A. Virosztek has led to a novel explanation of the anomalous frequency variation of the optical reflectivity as well as the Raman spectrum of high temperature superconductors. A key feature of this work is the presumed existence of nearly parallel "nested" sections of the Fermi surface. We found that electron-electron scattering across such nested regions yields an unusual linear frequency variation of the electron damping in contrast to textbook derivations of conventional Fermi liquid behavior. Explicit calculations of the dielectric function revealed a non-Drude reflectivity which fits the measured spectra of $YBa_2Cu_3O_7$ and $Bi_2SrCaCu_2O_8$ quite well. Our analysis of the Raman spectrum is based on light coupling to energy density fluctuations which yield a large light scattering cross section in situations with anisotropic energy bands. Remarkably good fits to the Raman lineshape of the above cuprates were achieved using the same electron-electron coupling that was established previously from the reflectivity analysis.

Since nested orbits are known to exist in chromium and some rare earth metals, it was gratifying to find some experimental evidence for non-Drude reflectivity curves in such materials also. Experimental groups are now measuring the Raman spectrum of rare earths to probe a frequency regime up to 1 eV for signs of a broad electronic continuum of the sort that was primary mystery in the copper oxide superconductors.

Dr. A. Virosztek continues his analysis and close interaction with our group from his permanent position in Budapest, Hungary and his extended visits to laboratories in Germany.

Research associate Dr. Jian Zhang focussed attention on a Boltzmann equation solution for the resistivity caused by electron-electron scattering across nested orbits and verified the linear temperature variation of the resistance in cases with substantial nesting. His estimates of the magnitude of the scattering agree with experimental data. Most recently, he initiated an analysis of the neutron spectra of the superconductors $La_{2-x}Sr_xCuO_4$ and $YBa_2Cu_3O_{6+x}$ which verified two controversial features of the electronic response. The scaling of the spin susceptibility as a function

of frequency divided by the temperature was predicted by our group for a simple idealistic nesting model and has been recently observed by neutron scattering measurements in Grenoble as well as by the MIT-Brookhaven group. We have now extended the analysis to a more realistic tight-binding energy band model which shows scaling features when the Fermi energy is close to half-filling, and also yields momentum scan lineshapes with a twin peak structure that agree in detail with data on $La_{2-x}Sr_xCuO_4$.

Dr. Carsten T. Rieck has just joined our group as a Research Associate and has already produced analytic derivations as well as computer generated response functions of a tight-binding model with variable nesting features. This research is directly relevant to the neutron spectra of high temperature superconductors and will be important for our future investigation of the nuclear magnetic response (NMR) of cuprates.

Graduate student Jeffrey Thoma has initiated his research with a study of the screening of the Coulomb interaction in the metallic phases of high temperature superconductors.

Time Devoted to Project by Principal Investigator

1. 50% of time during the academic year period September 1, 1991 - June 1, 1992.
2. 100% of time June 1, 1992 - August 31, 1992.
3. 50% of time during the forthcoming academic year period September 1, 1992 - Feb. 28, 1993.

Research Projects

Our research on high temperature superconductors has produced novel insights for the normal state properties of copper oxides that have been discovered in the last few years. Advances in materials preparation have produced single crystal samples, and sophisticated surface cleavage techniques have unveiled truly metallic behavior in many respects. Thus, the recent confirmation of a Fermi surface in several cuprate superconductors by photoemission spectroscopy has aroused interest in experimental features which heretofore were in apparent contrast to the expectations for a conventional Fermi Liquid.

Standard Fermi Liquid properties are based on well defined quasiparticles whose damping is small at the Fermi energy E_F. Ordinary metals such as copper are notable for very weak electron-electron contributions to the damping which barely influence the electrical resistivity or the optical response.

Our group has discovered that "nested" nearly parallel sections of the electron orbits yield an anomalous response which influences the electrical resistivity, optical reflectance, Raman spectrum, and neutron scattering cross section. Our analysis has provided an explanation for seemingly disparate experimental features of high temperature superconductors using consistent values for the electron-electron coupling and the plasma frequency. Our results include the following properties of high temperature superconductors:

I. Nested Fermi Liquid Response in High Temperature Superconductors

II. Optical Reflectivity and Electron Energy Loss Data

III. Raman Spectra

IV. Neutron Scattering Cross Section and Scaling

V. Prospects for New Superconductors.

I. NESTED FERMI LIQUID RESPONSE

A fundamental issue for high temperature superconductors is the apparent inadequacy of a conventional[1,2] Fermi liquid description for the transport data, such as the resistivity, optical properties, and other features. Yet photoemission measurements[3] on freshly cleaved single crystals provide convincing evidence for the existence of a Fermi surface and electronic bands with considerable dispersion.

We have discovered[4] a possible resolution of the Fermi Liquid dilemna as a consequence of "nesting" which refers to Fermi surfaces with sections that are nearly parallel in momentum space. Our calculations rely on a conventional Hamiltonian

$$H = \sum_{k\sigma} E(\vec{k})\, c^{+}_{k\sigma}\, c_{k\sigma} + U \sum_{i} n_{i\uparrow} n_{i\downarrow}, \tag{1}$$

where $U > 0$ denotes the on-site Coulomb repulsion, $c^{+}_{k\sigma}$ ($c_{k\sigma}$) are the creation (destruction) operators for an itinerant electron or hole within a band $E(\vec{k})$ of width W.

Electron scattering is limited by the Pauli exclusion principle to a narrow region of space for a fixed temperature T and distance from the Fermi energy E_F. Hence the topology of the electron orbit is a key determinant in the damping rate Γ caused by the electron-electron coupling.

A conventional Fermi liquid refers to an energy dispersion $E(\vec{k}) = k^2/2m^*$ with an effective mass m^*. In three dimensions, the standard damping [2] is

$$\Gamma_{FL} = \frac{\pi\alpha^2}{2W}\left[\pi^2 T^2 + \omega^2\right], \tag{2}$$

where T and W are in energy units and the dimensionless coupling is $\alpha = U/W$. This Born approximation result is justified because the damping is quite small in ordinary metals because the bandwidth is much larger than the typical temperatures of interest. Physically the variation $\Gamma_{FL} \sim T^2$ follows from the Pauli exclusion requirement that limits the states available for the incoming electron

to a shell of thickness T, and another factor of T comes from the restriction on the target electron.

Nesting of the Fermi surface refers to a quasiparticle orbit with nearly parallel sections separated by a nesting wave vector $\vec{Q}^*$. An example of a nested orbit is shown in Fig. 1; this example reverts to perfect nesting for a square orbit in the case of a half-filled tight-binding band in two dimensions. This situation is especially germane to the Cu $d_{x^2-y^2}$ orbitals in the Cu-0 plane structures found in high temperature superconductors.

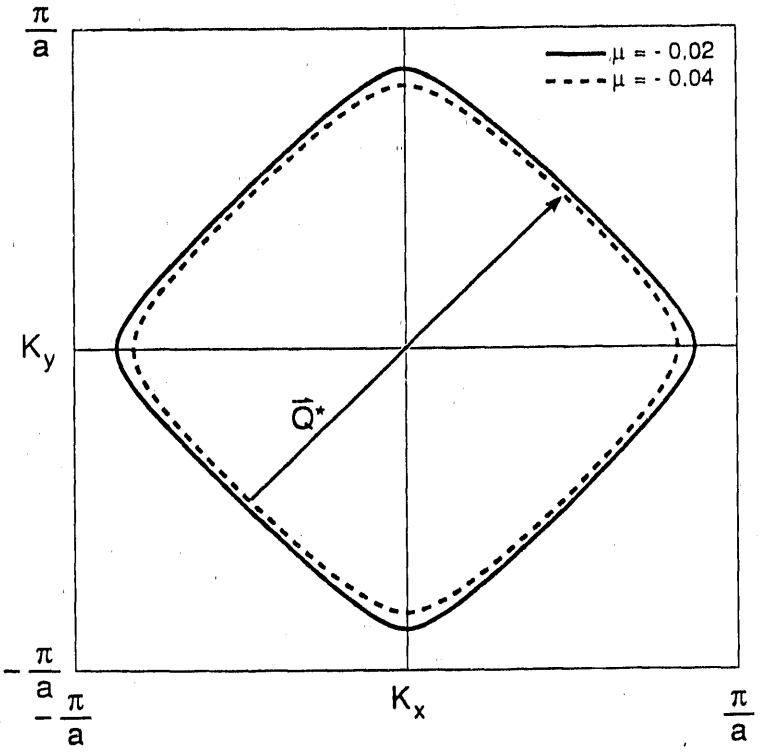

Fig. 1. Example of nesting corresponding to a wavevector $\vec{Q}^*$ for a nearly half-filled tight-binding energy band in two dimensions. Electron-electron across parallel sections of the Fermi surface is sensitive to the dimensionless Fermi energy $\mu = E_F/W$, and yields a divergent cross section in the limit $\mu = 0$ that corresponds to a square orbit with the ideal nesting at $\vec{Q} = (\pi, \pi)/a$.

Our initial calculations invoked the approximate nesting condition $E(\vec{k}+\vec{Q})+E(\vec{k})=0$, which yields an unusual damping rate caused by the dominance of scattering processes with

momentum $\vec{Q}$. The details of the analysis have just been published [4], and yield the following features for a nested Fermi Liquid (NFL). The solution for the quasiparticle damping is:

$$\Gamma_{NFL}(\omega \leq T) \sim \alpha T, \tag{3}$$

and

$$\Gamma_{NFL}(\omega \geq T) \sim \alpha \omega. \tag{4}$$

Direct experimental evidence[3] for the frequency variation $\Gamma_{NFL} = \alpha\omega$ has been discovered by photoemission spectroscopy on $Bi_2Sr_2CaCu_2O_8$ superconductors with $\alpha \sim 0.6$.

The magnitude of the quasiparticle damping Γ may be quite different from the transport relaxation rate which determines electrical conductivity. Scattering on a spherical orbit by normal processes conserves velocity, so that electron-electron collisions in this case give a vanishing contribution to the resistivity. By contrast, nested regions of an electron trajectory yield processes where the target electron can conserve momentum by scattering from state $\vec{k}$ to $\vec{k} + \vec{Q}$, but nevertheless may have a range of velocities depending on which point of the anisotropic Fermi surface the scattering originates. Hence large net changes in current and conductivity are possible for scattering between nested regions. We have derived solutions of the Boltzmann transport equation for simple models of nested surfaces and verified that the expected transport relaxation rate is indeed compatible with the measured resistivities of cuprates.

A more specific test of the transport relaxation rate is its frequency variation which dominates the optical conductivity which we discuss next.

II. OPTICAL PROPERTIES OF HIGH TEMPERATURE SUPERCONDUCTORS

Infrared reflectivity $R(\omega)$ measurements on single crystal specimens reveal a frequency variation in cuprates that is quite different from the classical Drude behavior found in ordinary metals like copper and silver. Typical examples are shown in Fig. 2 where the standard Drude form is exemplified by the Cu data[5] which shows a large smooth reflectivity up to the plasma frequency of several eV. By contrast the reflectivity spectra of the $Bi_2Sr_2CaCu_2O_8$ superconductor[6] and data[7] on untwinned $YBa_2Cu_3O_7$ shows a rapid decrease of the reflectivity over the frequency range up to 8000 cm^{-1} ≈ 1 eV. Curiously, the infrared response of metallic chromium[8] yields non-Drude behavior also, as seen in Fig. 2.

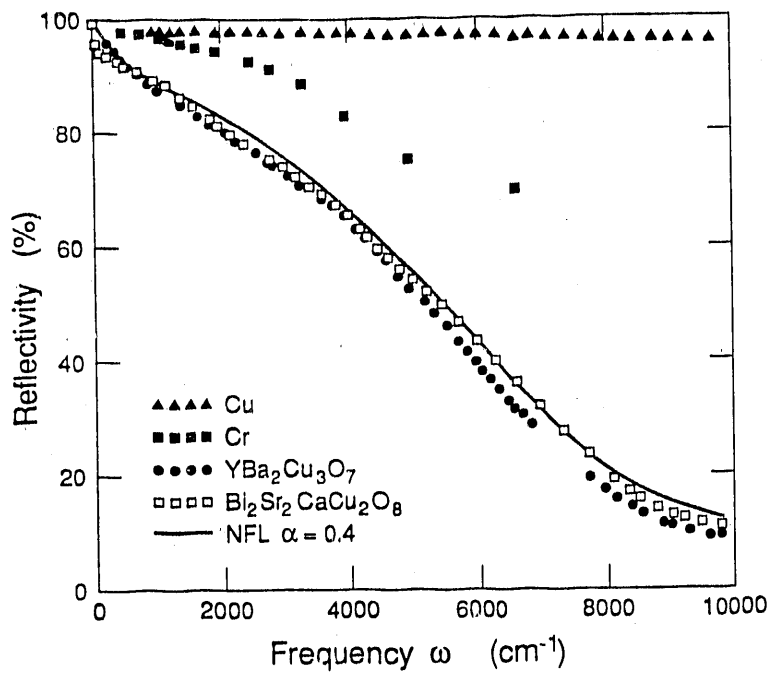

Fig. 2. Infrared reflectivity up to the 1 eV ≈ 8000 cm^{-1} energy range shows the standard Drude behavior for copper (Δ), in contrast to the anomalous decline for two high temperatures superconductors (●, □). The solid curve is our result for a nested Fermi surface with an electron-electron scattering strength $\alpha = 0.4$. Non-Drude behavior of Cr (■) is also seen.

Our calculations yield the solid curve shown in Fig. 1 with the details published this year.[9] The basic result for a nested Fermi surface is a modified dielectric function

$$\epsilon_{NFL}(\omega) = \epsilon_\infty - \frac{\omega_p^2}{\omega\left[\omega\frac{m^*_{NFL}}{m_0} + \frac{i}{\tau_{NFL}}\right]} \tag{5}$$

where consideration of self energy and vertex corrections yield a transport relaxation time τ_{NFL} given by

$$\frac{1}{\tau_{NFL}}(\omega<2T) = 3.3\alpha T \tag{6}$$

and

$$\frac{1}{\tau_{NFL}}(\omega>2T) = \alpha\omega \tag{7}$$

which are somewhat different from the Born Approximation result for the quasiparticle damping in Eqs. 3 & 4. To satisfy causality, the effective mass becomes frequency and temperature dependent:

$$m^*_{NFL} = m_0\left[1+\frac{2\alpha}{\pi}\ln\frac{\omega_c}{Max(2T,|\omega|)}\right], \tag{8}$$

where ω_c is a cut-off frequency constrained to be $\omega_c \leq W/(1+\alpha)$ for a bandwidth W.

Drude relaxation is described by a constant mass and relaxation time which works well for Cu but fails to describe cuprate reflectivity data as seen in Fig. 2.

An additional test of the theory is the low frequency region of the conductivity $\sigma(\omega)$ which checks the predicted temperature variation of the damping $1/\tau$. Extrapolating the conductivity to the DC limit $\omega=0$ yields a resistivity that is linear in temperature and has a magnitude in qualitative agreement with the observations.

A principal result of our analysis is information regarding the charge carrier density n which appears in the plasma frequency $\omega_p^2 = 4\pi ne^2/m_0$. To pin down this quantity more precisely we have

obtained the structure factor

$$S_{NFL}(q\sim 0,\omega) \sim \mathrm{Im}\left[\frac{-1}{\epsilon_{NFL}(\omega)}\right]. \qquad (9)$$

The computed structure shows in Figure 3 the Drude prediction as a narrow peak at low frequency determined by the fit to the reflectivity data. By contrast the nested case yields a much broader peak at a higher frequency, and it is gratifying that the electron loss measurements by the Karlsruhe group[10] reveal the broad features predicted by the NFL analysis using the same α and ω_p from our previous optical studies. Independent construction of the structure factor using the real and imaginary parts of the dielectric function deduced from the optical reflectivity yields even better agreement with our calculated structure factor in Figure 3.

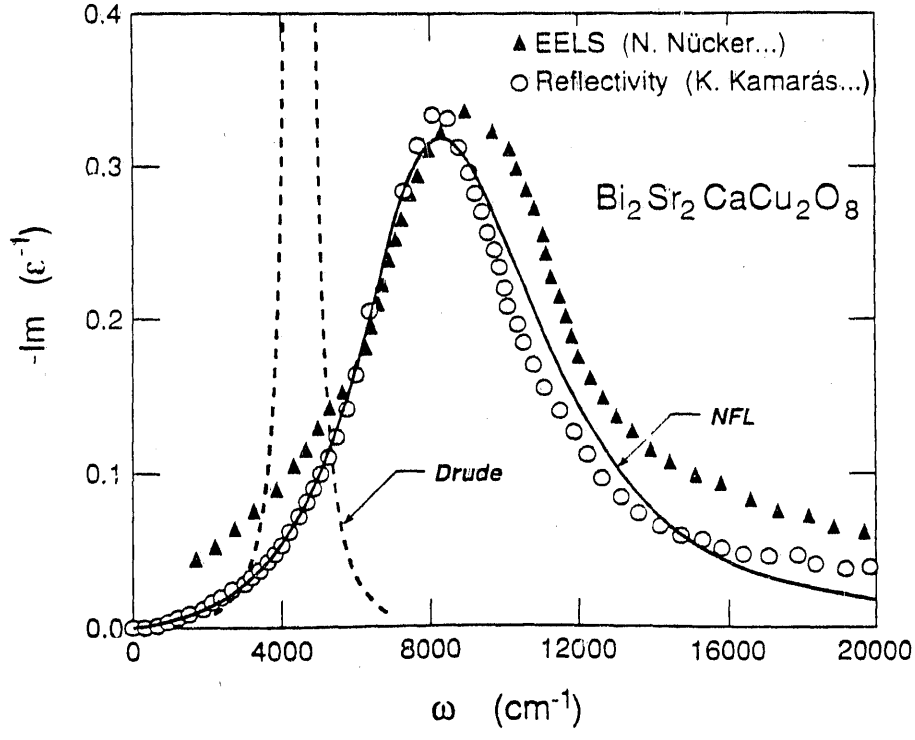

Fig. 3. Electron loss function for $Bi_2Sr_2CaCu_2O_8$ derived from optical data of Ref. 6 is shown by circles. The calculated NFL spectrum is in good accord with the low frequency and plasmon peak region using $\epsilon_\infty = 5$, $\omega_p = 3.1$ eV, $\alpha = 0.4$ and a cut-off $\omega_c = 1.4$ eV. The NFL conductivity and structure factor satisfy f-sum rules with these parameters and the anomalous plasmon width is caused by nesting. Electron loss data from Ref. 10 at q = 0.05 Å^{-1} yields a similar plasmon peak shifted slightly to higher frequency. A Drude fit of the low frequency conductivity predicts the much narrower peak shown by the dashed curve and a strong temperature variation of the width which also contrasts to the data.

Charge conservation imposes constraints which are satisfied by the formal development of our NFL theory.[9] Furthermore, direct numerical integration of the structure Factor in Fig. 3 demonstrates satisfaction of the f-sum rules and further supports the metallic character of the nested orbits predicted by band structure calculations,[11] and supported by photoemission spectroscopy.[12]

An apparent contradiction in estimates of the charge carrier density from Hall effect data may be resolved by the presence of hole orbits as well as a large nested electron orbit. The effects of strong electron-electron scattering among nested regions combined with topological influences on the velocity averages tend to drastically reduce the electron orbit contribution to the Hall current.[13] Explicit calculations for a simple nesting model demonstrate such competition in the Hall coefficient which follows the measured trend as a function of Sr content in $La_{2-x}Sr_xCuO_4$.

III. ELECTRONIC RAMAN SPECTRA

Raman scattering in metals with parabolic energy bands is expected to be weak. The light cross section is proportional to the Fermi-gas structure factor[2] $S(q,\omega)$ which vanishes at $q \to 0$ as a result of particle conservation. Consequently, the small momentum transfer q of the light makes single-particle or plasmon excitations exceedingly difficult to observe in ordinary metals.

Discoveries of broad electronic features[14,15] in $YBa_2Cu_3O_7$ and similar anomalies in other high-temperature superconductors generated much interest, in part because the smooth line shape extends to nearly 1 eV in some cases[16-18]. The spectra of the metallic oxides display intensities similar to the two-magnon scattering in the insulating oxides,[16] but the line shapes are much different, with a prominent peak in the case of the antiferromagnetic insulators.

An example of the anomalous spectrum[18] of single crystal $Bi_2Sr_2CaCu_2O_8$ is shown in Fig. 4.

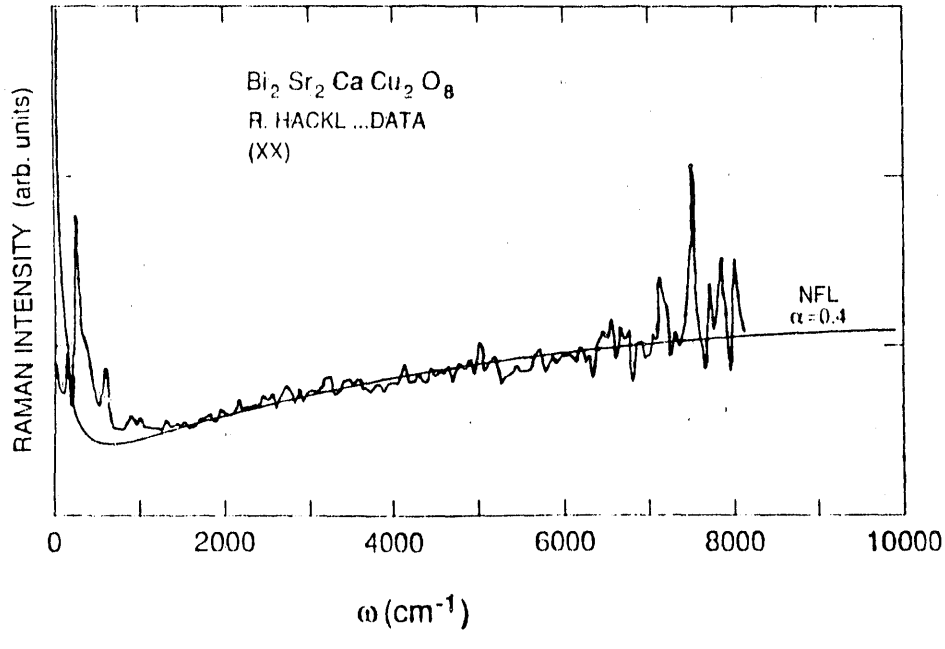

Fig. 4. Raman spectrum of $Bi_2Sr_2CaCu_2O_8$ from Ref. 18 is compared to the NFL line shape calculated using $\alpha = 0.4$ and $\omega_c = 1.4$ eV. These parameters are identical to the values which were found earlier in the NFL analysis of optical conductivity and also are compatible with the structure factor shown in Fig. 3 along with the f-sum rules.

Our calculated[19] Raman cross section is shown by the solid smooth curve which fits the data over a wide frequency range up to 1 eV = 8,000 cm.$^{-1}$ At frequencies below 1,000 cm^{-1} the phonon scattering interferes with electronic continuum and shows the expected asymmetric line shapes near the phonon peaks. We shall examine the coupling of phonons to the electronic scattering later.

The essence of our explanation for the Raman continuum is the nested Fermi liquid concept which may couple to the light via energy density fluctuations in anisotropic energy bands. In the absence of nesting, the energy density fluctuation scattering mechanism has been discussed in connection with doped semiconductors[20] and conventional superconductors. However, the latter materials exhibit Raman lineshapes that are quite different from the high temperature superconductors.

Details of our Raman calculation appeared in print last month and a longer descriptive treatment has just been accepted by Physical Review B.[22] The general features include a Raman cross section[23]

$$I_R = r_0^2 \left[1 - e^{\omega/T}\right]^{-1} \mathrm{Im}\, \tilde{\chi}\,(q, \omega), \tag{10}$$

where $r_0 = e^2/mc^2$ is the Thomson radius, and

$$\tilde{\chi}\,(q, \omega) = \langle [\tilde{\rho}, (q)\, \tilde{\rho}\,(-q)] \rangle\,(\omega) \tag{11}$$

describes energy-density fluctuations

$$\tilde{\rho}\,(q) = \sum_{k\sigma} \gamma\,(k)\, c^{+}_{k+q,\sigma}\, c_{k,\sigma} \tag{12}$$

in terms of the electron creation (destruction) operators $c^{+}_{k\sigma}$ ($c_{k\sigma}$). The nonparabolic E (k) band determines γ(k) and thus distinguishes $\tilde{\rho}$ from ordinary particle density operators.

After careful consideration of the NFL damping discussed in sections I & II of this report, and inclusion of vertex corrections, we found a Raman spectrum for nested Fermi surfaces of the form

$$I_{NFL} = r_0^2 N(0)\left[1 - e^{-\omega/T}\right]^{-1} \sum_{L\neq 0} \gamma_L^2 \frac{\omega\, \tau_{NFL}(\omega)}{\left[m^*_{NFL}(\omega)/m_0\right]^2 \omega^2 \tau^2_{NFL}(\omega) + 1}, \tag{13}$$

where the expansion $\gamma(k) = \sum_L \gamma_L \varphi_L(k)$ in terms of a complete set of surface harmonics $\varphi_L(k)$ determines the coefficients γ_L. This formula yields the theoretical NFL curve in Fig. 4 which provides a novel explanation for the cuprate data. Other examples of nested Fermi surfaces include rare earth metals and chromium. A broad electronic continuum has been observed in Raman data on Dy, Er, and Y films,[24] and further experimental tests of these NFL predictions are in progress at various laboratories.

IV. NEUTRON SCATTERING CROSS SECTION AND SCALING

Neutrons probe the spin susceptibility $\chi(\vec{q}, \omega)$ at low frequencies ω as a function of momentum $\vec{q}$. This technique therefore provides a sensitive test of nesting features that we have recently predicted.[9]

Recent neutron experiments[25-27] on large single crystals of $YBa_2Cu_3O_x$ and $La_{2-x}Sr_xCuO_4$ have verified the unusual scaling of the susceptibility as a function of ω/T in the vicinity of a nesting vector $\vec{Q}$. This scaling is easily derived for an idealized nesting condition by considering the imaginary part of the susceptibility

$$\chi_0''(\vec{q},\omega) = -\frac{1}{4\pi}\int d^2k\left\{f\left[E(\vec{k}+\vec{q})\right] - f\left[E(\vec{k})\right]\right\}\delta\left[\omega - E(\vec{k}+\vec{q}) + E(\vec{k})\right], \tag{14}$$

where $f(x)=[\exp(x/T)+1]^{-1}$ is the Fermi function. Using the nesting condition $E_{\vec{k}+\vec{Q}} = -E_{\vec{k}} = x$ to define an energy variable x, and performing the δ-function integration gives

$$\chi''_{NFL,0}(\vec{Q},\omega) = \frac{\pi N(O)}{2}\tanh\left(\frac{\omega}{4T}\right). \tag{15}$$

In addition to the strong temperature dependence and scaling in ω/T, the saturation at large ω and the large magnitude of the susceptibility at a specific nesting vector $\vec{Q}$ is much different from conventional[2] Fermi liquid behavior.

Two examples of neutron scattering evidence for the above behavior are presented in Figures 5 and 6, while more complete details are available in a preprint.[28] First we show the frequency variation and scaling found[25] in $YBa_2Cu_3O_{6.51}$, along with our calculated response in Fig. 5. The solid curve in Fig. 5 is the idealized nesting result of Eq. 15 which could fit the data by a suitable adjustment in the density of states N(0) at the Fermi energy.

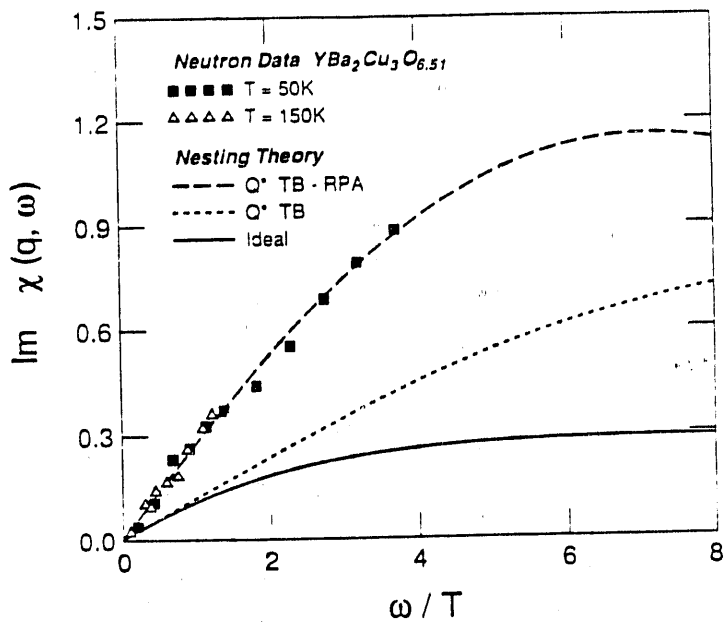

Fig. 5. Scaling of the imaginary part of the response function $\chi''(\vec{Q}^*, \omega)$, is shown by the neutron data on $YBa_2Cu_3O_{6.51}$ from Ref. (25) taken at two temperatures. The idealistic nesting model result of Eq. (15) is shown by the solid curve whereas the calculated tight binding model susceptibility at $aQ^* = 0.984$ (π, π) is shown by the dotted line for $\mu = E_F/W = -0.02$ and bandwidth $W = 8t = 2$ eV. The RPA corrections yield the enhanced (dashed) curve for $J = 0.069$ W.

A more realistic model that we have recently examined is a standard two dimensional tight-binding (TB) energy band

$$E(\vec{k}) = -2t\left[\cos(ak_x) + \cos(ak_y)\right] - E_F. \tag{16}$$

This model exhibits perfect nesting of a square Fermi surface for $E_F/8t=\mu=0$ at the ideal nesting vector $\vec{Q} = (\pi/a, \pi/a)$ where a is the lattice spacing. That special case yields a logarithmic singularity in the density of states and is unstable toward the formation of a spin density wave (SDW) for arbitrarily weak Coulomb repulsion. However, lowering the Fermi energy μ yields orbits with partial nesting characterized by a wavevector $Q^* < Q$ as shown in Figure 1, and these nesting features resemble the results of sophisticated band structure calculations for the cuprates[11] even though the value of Q^* may vary for different cuprates.

A numerical evaluation of the spin susceptibility for this TB model with the random phase[2]

approximation (RPA),

$$\chi''_{RPA}(\vec{q},\omega) = \frac{\chi''_0(\vec{q},\omega)}{\left[1 - J\chi'_0(\vec{q},\omega)\right]^2 + \left[J\chi''_0(\vec{q},\omega)\right]^2}, \tag{17}$$

yields the dotted and dashed curves in Fig. 5. The effective Coulomb coupling J estimated from the neutron data indicates strong screening of the on-site Coulomb repulsion by conduction electrons.

Confirmation of the NFL saturation at large ω is found[27] in the q-integrated neutron intensity for $La_{1.86}Sr_{.04}Cu0_4$, whereas the measured low frequency response scales with ω/T.

Another consequence of nesting is twin peak structure in the momentum variation of the susceptibility as a function of momentum near the nesting vector $\vec{Q}^*$. Our calculated spectrum for the TB model reveals structure that is remarkably similar to the neutron data[26] of $La_{1.86}Sr_{.14}Cu0_4$ as shown in Fig. 6.

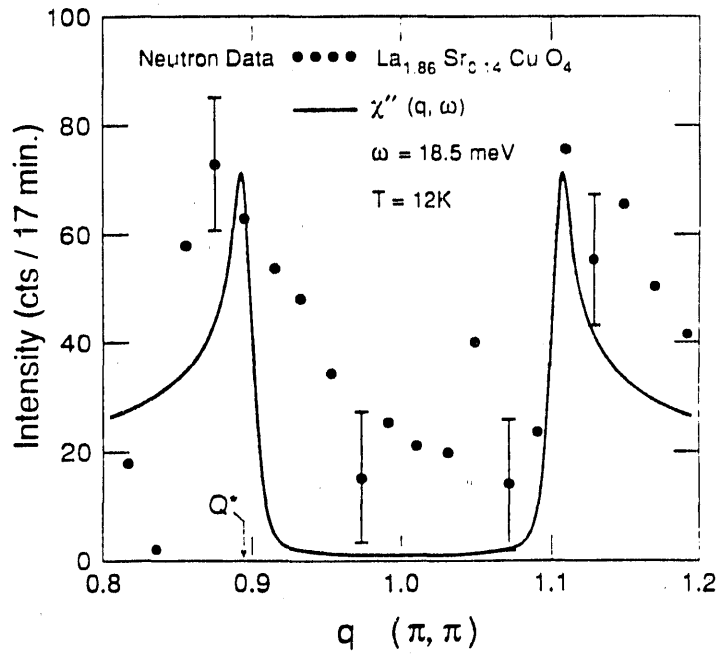

Fig. 6. Momentum variation of the neutron scattering data on $La_{1.86}Sr_{0.14}Cu0_4$ from Ref. 26 is compared to the calculated response including RPA corrections from Eq. 16. The model nesting wave vector $\vec{Q}^*$ refers to the peak position. At a frequency ω = 18.5 meV and a temperature T = 12 K, the separation of the twin peaks is achieved with Fermi energy μ = - 0.04 and bandwidth W = 2 eV. The proper peak height and lineshape is achieved with J = 0.069 W. Scans along q_x and other directions map regions of Fermi surface nesting which create the twin peaks.

Encouraged by the recent availability of neutron spectroscopy data on high temperature superconductors, we are extending these calculations to other momentum regions and including self-energy and higher-order corrections. From a physical point of view, it is interesting that the neutron spectrum of chromium[29] displays many similarities to the peak structure discovered in high temperature superconductors. Thus, an itinerant electron (or hole) description of the spin dynamics appears to provide a good foundation for the electronic structure of the superconducting cuprates.

V. PROSPECTS FOR NEW SUPERCONDUCTORS

Encouraged by our theoretical results, we have joined chemists and synthesized a variety of oxide and sulfide alloys with promising electronic structures for high temperature superconductivity. The remarkable enthusiasm and dedicated work of ten undergraduate students that have participated in our group during the last three years have provided a superb educational experience in an ambiance of pure discovery. Our student team included three women, including two minority students.

Laboratory facilities for our synthesis and sample characterization studies were provided by Dr. E. Sinn in our Chemistry department and by Prof. B. Farmer in our Materials Science department.

Most of the sample preparation was by vapor transport methods at high temperatures for the sulfides. Oxide preparation followed standard techniques reported in recent literature. Single phase properties were determined by x-ray diffraction and the onset of superconductivity was measured using a SQUID magnetometer which also yields the fraction of the sample that is superconducting from the measured Meissner effect.

A high point of our students' experience was the discovery[30] by chemistry graduate student Tom Sutto of a new superconducting alloy with composition $Ba_4Tl_{2-\delta}Bi_xPb_2O_{12-\delta}$. Although the maximum observed superconducting temperature was only $T_C = 10.7$ for $x = 1.0$, the concentration dependence of T_C is unusual. Measurements of the Pauli susceptibility of these alloys shows that T_C did not increase in correspondence to the electronic density of states. Powder x-ray studies reveal an orthophombic distortion in superconducting samples, whereas a tetragonal structure with alternating MO_2 layers (M = Tl,Bi,Pb) interspersed by Ba is evident for $x < 0.7$ and $x > 1.2$. Confirmation of the superconductivity was provided by resistance measurements with the aid of J. Poon's group in the Physics Department.

This interdisciplinary effort to synthesize novel alloys has been particularly interesting and valuable for student morale and experience. Previous experiments on a wide variety of sulfides were able to determine superconductivity at relatively low temperatures, and variations in composition of such alloys found by our group verified changes in the transition temperature that may be expected

for systems with a single band that comply with the BCS theory. However, our ultimate quest is to discover an appropriate chemical substitution in a layered sulfide compound that generates the partial filling of two electronic states with one of them near half filling in correspondence to the evidence for such a nesting condition in cuprates. Such a situation would provide a test of our theoretical basis for high T_C superconductivity and may result in new superconducting materials that are ductile and easier to use in commercial applications.

References

1. J.M. Luttinger, Phys. Rev. 121, 942 (1961).
2. "**The Theory of Quantum Liquids**," D. Pines and P. Nozieres, (Benjamin, NY, 1966).
3. C.G. Olson, R. Liu, D.W. Lynch, R.S. List, A.J. Arko, B.W. Veal, Y.C. Chang, P.Z. Jiang and A.P. Paulikas, Phys. Rev. B 42, 381 (1990).
4. A. Virosztek and J. Ruvalds, Phys. Rev. B42, 4064 (1990).
5. H. Bispinck, Z. Naturforsch, A25, 70 (1970).
6. K. Kamarás, et al., Springer Series in Solid-State Sciences 99, 260 (1990).
7. Z. Schlesinger, et al., Phys. Rev. Lett. 65, 801 (1990).
8. A. S. Barker, Jr. and J. A. Ditzenberger, Phys. Rev. B1, 4378 (1970).
9. J. Ruvalds and A. Virosztek, Phys. Rev. B43, 5498 (1991).
10. N. Nücker et al., Phys. Rev. B39, 12379 (1989).
11. J. Yu, A. J. Freeman, and J. H. Xu, Phys. Rev. Lett. 58, 1035 (1987).
12. J. C. Campuzano et al., Phys Rev. Lett. 64, No. 19, 2308 (1990).
13. J. Ruvalds and A. Virosztek, Phys. Rev. B42, 399 (1990).
14. S. L. Cooper, F. Slakey, M. V. Klein, J. P. Rice, E. D. Bukowski, and D. M. Ginsberg, Phys. Rev. B38, 11934 (1988).
15. F. Slakey, S. L. Cooper, M. V. Klein, J. P. Rice, and D. M. Ginsberg, Phys. Rev. B39, 2781 (1989).
16. K. B. Lyons and P. A. Fleury, J. Appl. Phys. 64, 6075 (1988).
17. S. Sugai, Y. Enomoto, and T. Murakami, Solid State Commun. 72, 1193 (1989).
18. T. Staufer, R. Hackl, and P. Müller, Solid State Commun. 75, 975 (1990); R. Hackl (unpublished).
19. A. Virosztek and J. Ruvalds, Phys. Rev. Lett. 67, 1657 (1991).
20. P. A. Wolff, Phys. Rev. 171, 436 (1968).
21. A. A. Abrikosov and V. M. Genkin, Zh. Eksp. Teor. Fiz. 65, 842 (1973). [Sov. Phys. JETP 38, 417 (1974)].
22. A. Virosztek and J. Ruvalds, Phys. Rev. B Jan. 1 (1992).
23. M. V. Klein and S. B. Dierker, Phys. Rev. B29, 4976 (1984).

24. R. T. Demers, S. Kong, M. V. Klein, R. Du, and C. P. Flynn, Phys. Rev. B38, 11523 (1988).

25. J. Rossat-Mignod, et al. Physica B169, 58 (1991).

26. S. W. Cheong, et al., Phys. Rev. Lett. 67 1791 (1991).

27. R. Keimer et al. Phys. Rev. Lett. 67, 1930 (1991).

28. J. Ruvalds, C. T. Rieck, J. Zhang, and A. Virosztek, submitted to Phys. Rev. Letters.

29. E. Fawcett, S. A. Werner, A. Goldman, and G. Shirane, Phys. REv. Lett. 61, 558 (1988).

30. T. E. Sutto, B. A. Averill and J. Ruvalds, Chemistry of Materials 3, 209 (1991).

preprint and reprints removed.